Electronic Supplementary Material (ESI) for Dalton Transactions.
This journal is © The Royal Society of Chemistry 2018

SUPPORTING INFORMATION

Reactivity of a dearomatised pincer $Co^{II}Br$ complex with PNC^{NHC} donors: alkylation and Si-H bond activation via metal-ligand cooperation

Thomas Simler,*[,a,b] Sylvie Choua,[c] Andreas A. Danopoulos,*[,a,d,e] Pierre Braunstein*[,a]

[a] Université de Strasbourg, CNRS, CHIMIE UMR 7177, Laboratoire de Chimie de Coordination, 4 rue Blaise Pascal, CS 90032, 67081 Strasbourg, France.

[b] current address: Institute for Inorganic Chemistry, KIT, Engesserstr. 15, 76131 Karlsruhe, Germany

[c] Université de Strasbourg, CNRS, CHIMIE UMR 7177, Propriétés Optiques et Magnétiques des Architectures Moléculaires, 4 rue Blaise Pascal, CS 90032, 67081 Strasbourg, France.

[d] Institute for Advanced Study (USIAS), Université de Strasbourg (France)

[e] Laboratory of Inorganic Chemistry, National and Kapodistrian University of Athens, Panepistimiopolis Zografou, Athens GR 15771, Greece

E-mail: thomas.simler@kit.edu, braunstein@unistra.fr, danopoulos@unistra.fr

Contents

I. SYNTHESIS AND CHARACTERISATION

I.1. General considerations

All air- and moisture-sensitive manipulations were performed under dry Ar atmosphere using standard Schlenk techniques or under N_2 in an MBraun glove-box, unless otherwise stated. Diethyl ether was dried by refluxing over sodium/benzophenone ketyl and distilled under an argon atmosphere prior use. Other solvents (pentane and toluene) were dried by passing through columns of activated alumina and subsequently purged with argon. These solvents were stored, after drying, over potassium mirror until use. C_6D_6 and toluene-d_8 were distilled over KH and degassed by freeze-pump-thaw cycles. The synthesis of [Co(^{Cy}P*N$_a$C^{NHC})Br] (**1**) has been described previously.[1]

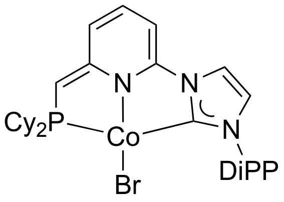

[Co(^{Cy}P*N$_a$C^{NHC})Br] (**1**)

Solid $LiCH_2SiMe_3$ was obtained from commercial solutions (Aldrich) by evaporation of the pentane under vacuum. All other chemicals were obtained from commercial sources and used without further purification.

NMR spectra were recorded on Bruker spectrometers (AVANCE III – 400 MHz or AVANCE I – 500 MHz equipped with a cryogenic probe). Downfield shifts are reported in ppm as positive and referenced using signals of the residual protio solvent (^1H), the solvent (^{13}C) or externally (^{31}P). All NMR spectra were measured at 298 K, unless otherwise specified. The multiplicity of the signals is indicated as s = singlet, d = doublet, t = triplet, sept = septet, m = multiplet and br = broad. Assignments were determined on the basis of unambiguous chemical shifts, coupling patterns and ^{13}C-DEPT experiments or 2D correlations (^1H-^1H COSY, ^1H-^{13}C HSQC). EPR spectra were recorded on a Bruker ESP300 spectrometer operating at X-band (9.4 GHz) with a standard rectangular cavity (TE102). An ESR900 cryostat (Oxford Instruments) was used for the low temperature measurements. Sample solutions in quartz tubes were prepared in a glove box. Elemental analyses were performed by the “Service de microanalyses”, Université de Strasbourg.

I.2. Synthesis of 3

I.2.1. Synthetic procedure

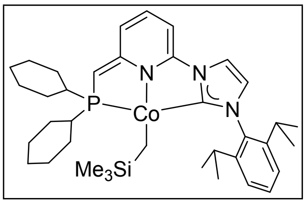

To a solution of [Co(^{Cy}P*N$_a$C^{NHC})Br] (**1**) (0.066 g, 0.10 mmol) in toluene precooled at -40 °C was added a cold solution of LiCH$_2$SiMe$_3$ (0.010 g, 0.10 mmol) in toluene. The resulting dark-purple solution was allowed to reach r.t. and stirred for 2 h. Filtration, evaporation of the solution and recrystallization from Et$_2$O afforded **3** as a dark purple solid. Yield of the crystals: 0.023 g (0.035 mmol), 35%. Single crystals suitable for X-ray crystallography studies were obtained by slow evaporation of a pentane solution of the complex.

The low isolated yield of **3** was due to its high solubility in common low polar solvent but ^{1}H NMR monitoring of the reaction indicated the clean conversion of **1** to **3**.

Satisfactory elemental analysis data could not be obtained but the purity of the compound can be assessed from its NMR spectra (see Fig S2).

^{1}H NMR (400.13 MHz, C$_6$D$_6$): δ 80.0 (2H, $\Delta\nu_{1/2}$ = 2000 Hz), 47.6 (2H, $\Delta\nu_{1/2}$ = 500 Hz), 40.5 (1H, $\Delta\nu_{1/2}$ = 110 Hz), 26.9 (1H, $\Delta\nu_{1/2}$ = 130 Hz), 26.4 (2H, $\Delta\nu_{1/2}$ = 800 Hz), 20.3 (2H, $\Delta\nu_{1/2}$ = 260 Hz), 13.5 (2H, $\Delta\nu_{1/2}$ = 52 Hz), 12.8 (2H, $\Delta\nu_{1/2}$ = 550 Hz), 11.2 (6H, $\Delta\nu_{1/2}$ = 42 Hz, CH(C*H*$_3$)$_2$), 9.6 (2H, $\Delta\nu_{1/2}$ = 58 Hz), 8.5 (3H, $\Delta\nu_{1/2}$ = 40 Hz), 6.8 (*ca.* 2H, $\Delta\nu_{1/2}$ = 800 Hz), 4.6 (2H, $\Delta\nu_{1/2}$ = 22 Hz), 2.8 (4H, $\Delta\nu_{1/2}$ = 45 Hz), 1.9 (2H, $\Delta\nu_{1/2}$ = 48 Hz), -2.3 (2H, $\Delta\nu_{1/2}$ = 590 Hz), -3.8 (1H, $\Delta\nu_{1/2}$ = 20 Hz), -10.7 (6H, $\Delta\nu_{1/2}$ = 75 Hz, CH(C*H*$_3$)$_2$), -18.1 (9H, $\Delta\nu_{1/2}$ = 115 Hz, SiMe$_3$), -25.2 (1H, $\Delta\nu_{1/2}$ = 120 Hz), -25.5 (1H, $\Delta\nu_{1/2}$ = 130 Hz), -52.0 (1H, $\Delta\nu_{1/2}$ = 350 Hz) (after baseline correction using the 'spline' mode).

I.2.2. Determination of the magnetic susceptibility

The determination of the magnetic susceptibility was carried out using Evans' method[2] for a C$_6$D$_6$ solution of **3** (0.0122 g, 18.5 μmol) containing toluene as internal reference and using a capillary of toluene as a diamagnetic standard. The solvent correction was not applied[3] and the diamagnetic corrections were calculated using Pascal's constants.[4] The ^{1}H-NMR spectrum was recorded at 400.13 MHz and 298 K. μ_{eff} = 2.2±0.1 $\mu_{B.}$

I.3. Synthesis of 4

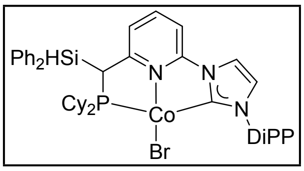

To a solution of [Co(^{Cy}P*N$_a$C^{NHC})Br] (**1**) (0.085 g, 0.13 mmol) in toluene precooled at -40 °C was added diphenylsilane (100 μL, 99 mg, 0.54 mmol). The resulting dark-purple solution was allowed to reach r.t. and stirred for 4 days, during which time it gradually turned dark green. After evaporation of the volatiles under vacuum, the resulting solid was extracted with Et$_2$O, filtered and washed with pentane, affording **4** as a dark green solid. Yield of the crystals: 0.018 g (0.022 mmol), 17%. Single crystals suitable for X-ray crystallography studies were obtained by slow evaporation of an Et$_2$O solution of the complex.

Satisfactory elemental analysis data could not be obtained but the purity of the compound can be assessed from its NMR spectra (see Fig S3-S7).

^{1}H NMR (500.13 MHz, C$_6$D$_6$): δ 8.80 (t, $^3J_{HH}$ = 7.6 Hz, 1H, *p*-C*H*$_{pyr.}$), 7.82-7.75 (m, 2H, C*H*$_{SiPh}$), 7.64-7.56 (m, 2H, C*H*$_{SiPh}$), 7.44 (t, $^3J_{HH}$ = 7.7 Hz, 1H, *p*-C*H*$_{DiPP}$), 7.34 (2 overlapping d, $^3J_{HH}$ = 8.1, 7.3 Hz, 2H, *m*-C*H*$_{DiPP}$), 7.24-7.18 (m, 3H, C*H*$_{SiPh}$), 7.05 (t, $^3J_{HH}$ = 7.4 Hz, 1H, C*H*$_{SiPh}$), 6.99 (t, $^3J_{HH}$ = 7.2 Hz, 2H, C*H*$_{SiPh}$), 6.93 (d, $^3J_{HH}$ = 2.0 Hz, 1H, C*H*$_{imid.}$), 6.82 (d, $^3J_{HH}$ = 2.0 Hz, 1H, C*H*$_{imid.}$), 6.36 (d, $^3J_{HH}$ = 7.4 Hz, 1H, *m*-C*H*$_{pyr.}$), 5.59 (s with d satellites $^1J_{SiH}$ = 203 Hz, 1H, Si*H*), 5.16 (d, $^3J_{HH}$ = 7.8 Hz, 1H, *m*-C*H*$_{pyr.}$), 4.06 (s, 1H, C*H*P), 3.79 (sept, $^3J_{HH}$ = 6.9 Hz, 1H, C*H*(CH$_3$)$_2$), 3.67 (sept, $^3J_{HH}$ = 6.9 Hz, 1H, C*H*(CH$_3$)$_2$), 2.83-2.67 (m, 1H, Cy), 2.60-2.45 (m, 2H, Cy), 2.26 (d, $^2J_{PH}$ = 12.9 Hz, 1H, Cy), 2.13 (d, $^2J_{PH}$ = 13.1 Hz, 1H, Cy), 2.02-1.75 (m, 4H, Cy), 1.70-1.36 (m, 7H, Cy), 1.63 (d, $^3J_{HH}$ = 6.9 Hz, 3H, CH(C*H*$_3$)$_2$), 1.59 (d, $^3J_{HH}$ = 6.9 Hz, 3H, CH(C*H*$_3$)$_2$), 1.30 (d, $^3J_{HH}$ = 6.9 Hz, 3H, CH(C*H*$_3$)$_2$), 1.29 (d, $^3J_{HH}$ = 6.9 Hz, 3H, CH(C*H*$_3$)$_2$), 1.23-1.00 (m, 5H, Cy), 0.97-0.84 (m, 1H, Cy) ppm.

^{13}C{^{1}H} NMR (125.77 MHz, C$_6$D$_6$): δ (C$_{NHC}$ not detected) 159.0 (*C*$_{arom.}$), 145.6 (d, J_{PC} = 1.6 Hz, *C*$_{arom.}$), 143.2 (*C*$_{arom.}$), 139.4 (*C*$_{arom.}$), 136.2 (*C*H$_{SiPh}$), 135.9 (*C*H$_{SiPh}$), 134.6 (*C*$_{arom.}$), 131.8 (*C*$_{arom.}$), 130.3 (d, J_{PC} = 7.5 Hz, *C*H$_{SiPh}$), 129.7 (*C*H$_{DiPP}$), 128.7 (*C*H$_{SiPh}$), 128.6 (*C*H$_{imid.}$), 128.4 (*C*H$_{SiPh}$), 123.9 (*m*-*C*H$_{DiPP}$), 123.8 (*m*-*C*H$_{DiPP}$), 123.5 (*m*-*C*H$_{pyr.}$), 112.5 (*m*-*C*H$_{pyr.}$), 112.1 (*p*-*C*H$_{pyr.}$), 110.7 (*C*H$_{imid.}$), 37.5 (*C*HP), 34.0 (*C*H$_{Cy}$), 331 (*C*H$_{Cy}$), 30.7 (d, J_{PC} = 25.1 Hz, *C*H$_{2\ Cy}$), 29.5 (*C*H(CH$_3$)$_2$), 29.3 (*C*H(CH$_3$)$_2$), 29.1 (d, J_{PC} = 27.5 Hz, *C*H$_{2\ Cy}$), 27.8 (*C*H$_{2\ Cy}$), 27.5 (*C*H$_{2\ Cy}$), 24.6 (*C*H$_{2\ Cy}$), 27.0 (*C*H$_{2\ Cy}$), 26.8 (*C*H$_{2\ Cy}$), 26.4 (*C*H$_{2\ Cy}$), 25.4 (CH(*C*H$_3$)$_2$), 25.2 (CH(*C*H$_3$)$_2$), 24.3 (CH(*C*H$_3$)$_2$), 24.1 (CH(*C*H$_3$)$_2$) ppm.

^{31}P{^{1}H} NMR (161.98 MHz, C$_6$D$_6$): δ 74.4 (br s) ppm.

II. X-RAY CRYSTALLOGRAPHY

II.1. General methods

Suitable crystals for the X-ray analysis of all compounds were obtained as described above. Summary of the crystal data, data collection and refinement for compounds are given in Table S1. Data sets were collected at 173(2) K on a Bruker APEX-II CCD Duo diffractometer (graphite-monochromated Mo-Kα radiation, λ = 0.71073 Å). Specific comments for each data set are given below.

The cell parameters were determined (APEX2 software)[5] from reflections taken from three sets of 12 frames, each at 10 s exposure. The structures were solved by direct methods using the program SHELXS-2013.[6] The refinement and all further calculations were carried out using SHELXL-2013.[6b] The H-atoms were introduced into the geometrically calculated positions (SHELXL-2013 procedures) unless stated otherwise and refined riding on the corresponding parent atoms. The non-H atoms were refined anisotropically, using weighted full-matrix least-squares on F^2.

The following special comments apply to the model of **4**:

- The configuration of the asymmetric carbon atom C21 in Fig. 4 (main text) is *R*. The space-group $P2_1/c$ being centrosymmetric, both enantiomers are present in the unit cell. The hydrogen on the silicon atom has been located (and not placed on a calculated position).

II.2. Summary of crystal data

Table S1. Crystal data, data collection and refinement for compounds **3**-**4.**

Compounds	**3**	**4**
Chemical formula	$C_{37}H_{56}CoN_3PSi$	$C_{45}H_{56}BrCoN_3PSi$
CCDC Number	1834127	1834128
Formula Mass	660.83	836.82
Crystal system	Monoclinic	Monoclinic
a/Å	10.5003(13)	13.8439(6)
b/Å	13.9842(17)	17.8666(8)
c/Å	24.484(3)	16.9012(7)
α/°	90	90
β/°	90.618(3)	93.1540(10)
γ/°	90	90
Unit cell volume/Å^3	3595.1(8)	4174.1(3)
Temperature/K	173(2)	173(2)
Space group	$P2_1/c$	$P2_1/c$
No. of formula units per unit cell, Z	4	4
Absorption coefficient, μ/mm	0.584	1.470
No. of reflections measured	72387	89251
No. of independent reflections	12458	14505
R_{int}	0.0388	0.0318
Final R_1 values ($I > 2\sigma(I)$)	0.0443	0.0486
Final $wR(F^2)$ values ($I > 2\sigma(I)$)	0.0928	0.1116
Final R_1 values (all data)	0.0656	0.0725
Final $wR(F^2)$ values (all data)	0.1032	0.1265
Goodness of fit on F^2	1.030	1.079

III. NMR SPECTRA

III.1. Evolution from 2 to 1 upon heating

The crude product obtained after reaction of $(^{Cy}PN^{pyr}C^{im})Br$ with $[Co\{N(SiMe_3)_2\}_2]$ in THF at room temperature was dissolved in toluene-d_8 and placed in a Young NMR tube. The mixture was heated to 110 °C and the reaction was monitored by ^1H NMR, revealing conversion of $[Co(^{Cy}PN^{pyr}C^{NHC})\{N(SiMe_3)_2\}Br]$ (**2**) into $[Co(^{Cy}P{*}N^{a}C^{NHC})Br]$ (**1**) and $HN(SiMe_3)_2$.

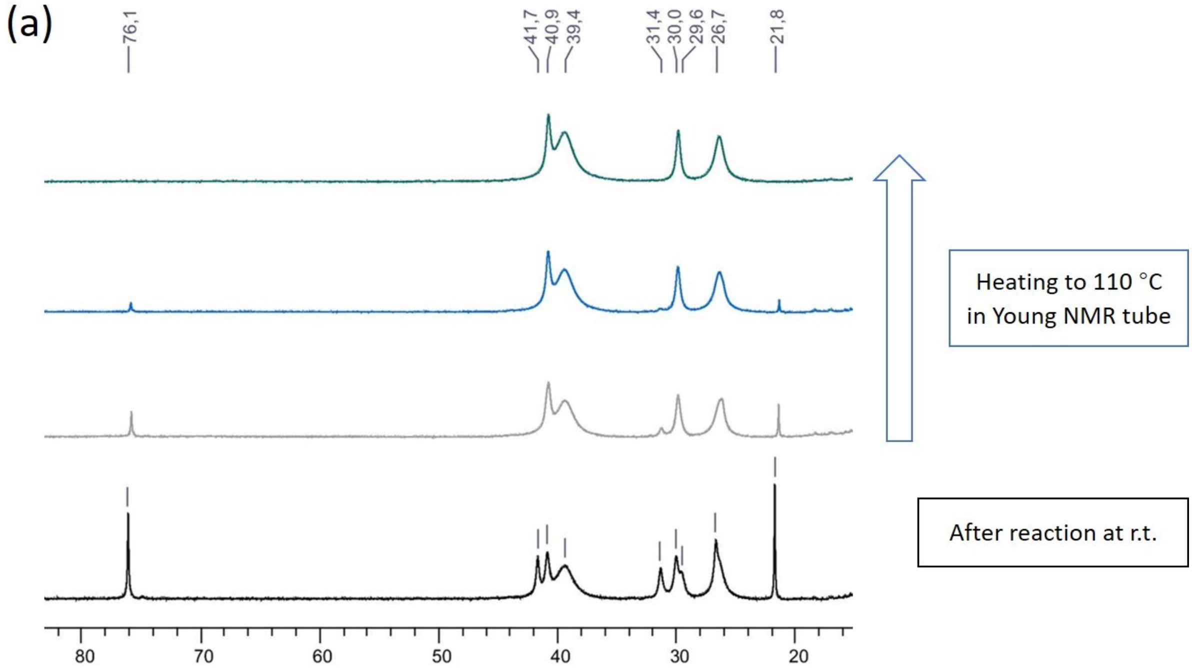

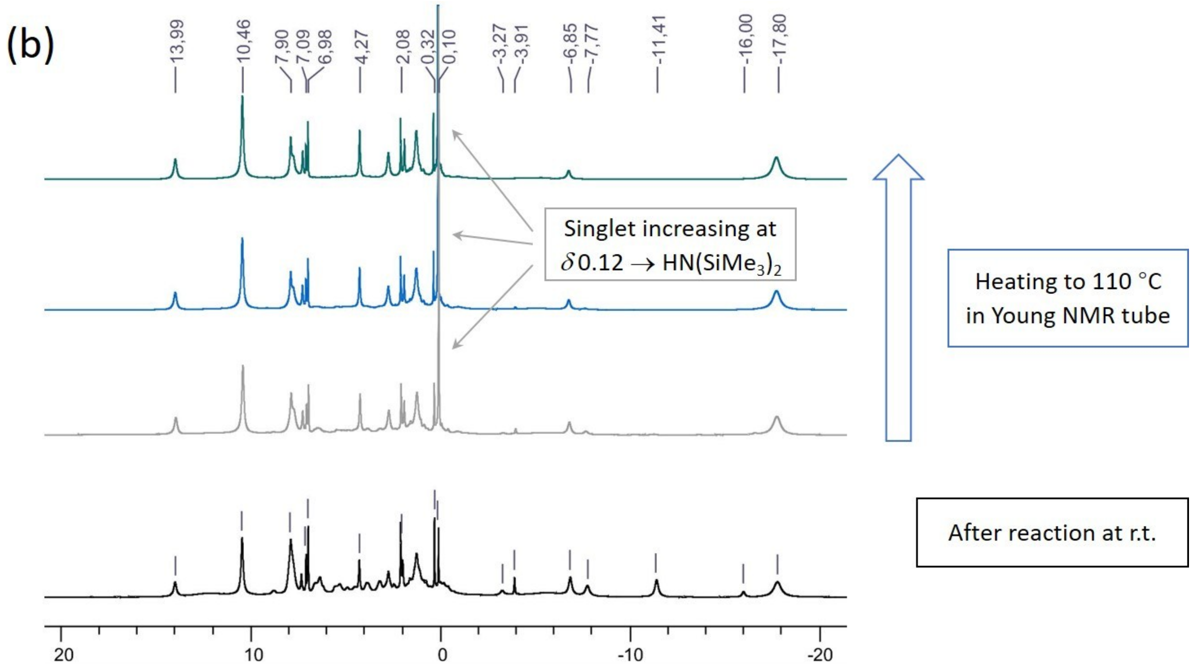

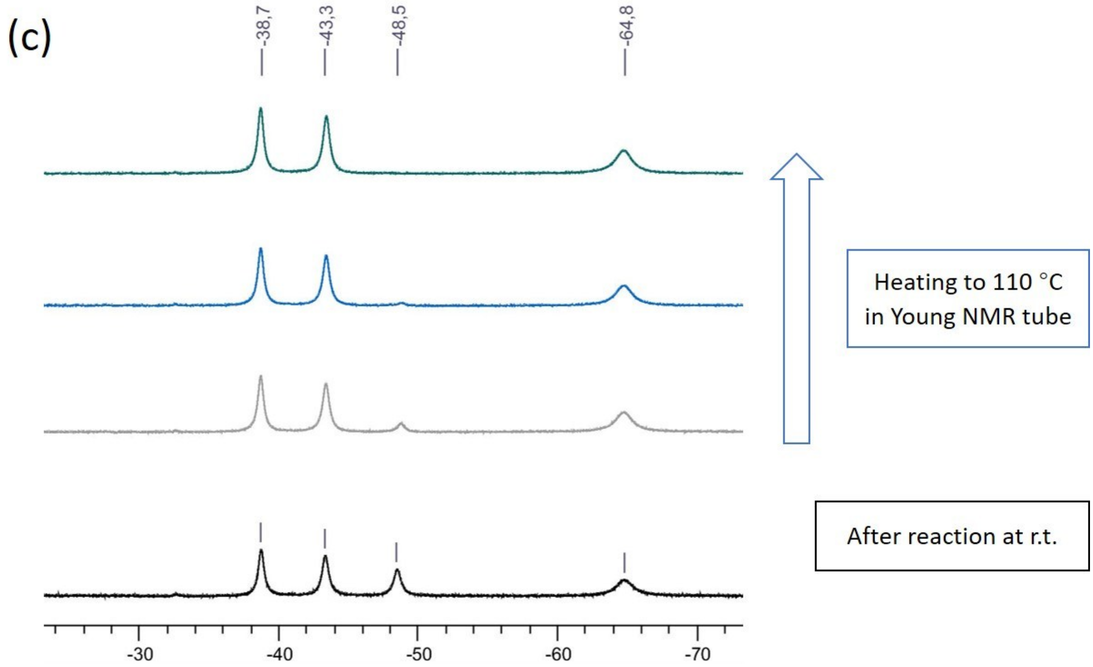

Figure S1. Evolution of the ^{1}H NMR spectrum upon heating to 110 °C in toluene-d_8 (detail from δ 80 to 20 ppm (a), from δ 20 to -20 ppm (b) and from δ -20 to -75 ppm (c)). Residual [Co($^{\mathbf{Cy}}$PN^{pyr}C^{NHC}){N(SiMe$_3$)$_2$}Br] (**2**) converts into [Co(^{Cy}P*N^{a}C^{NHC})Br] (**1**) and HN(SiMe$_3$)$_2$.

III.2. Complex 3

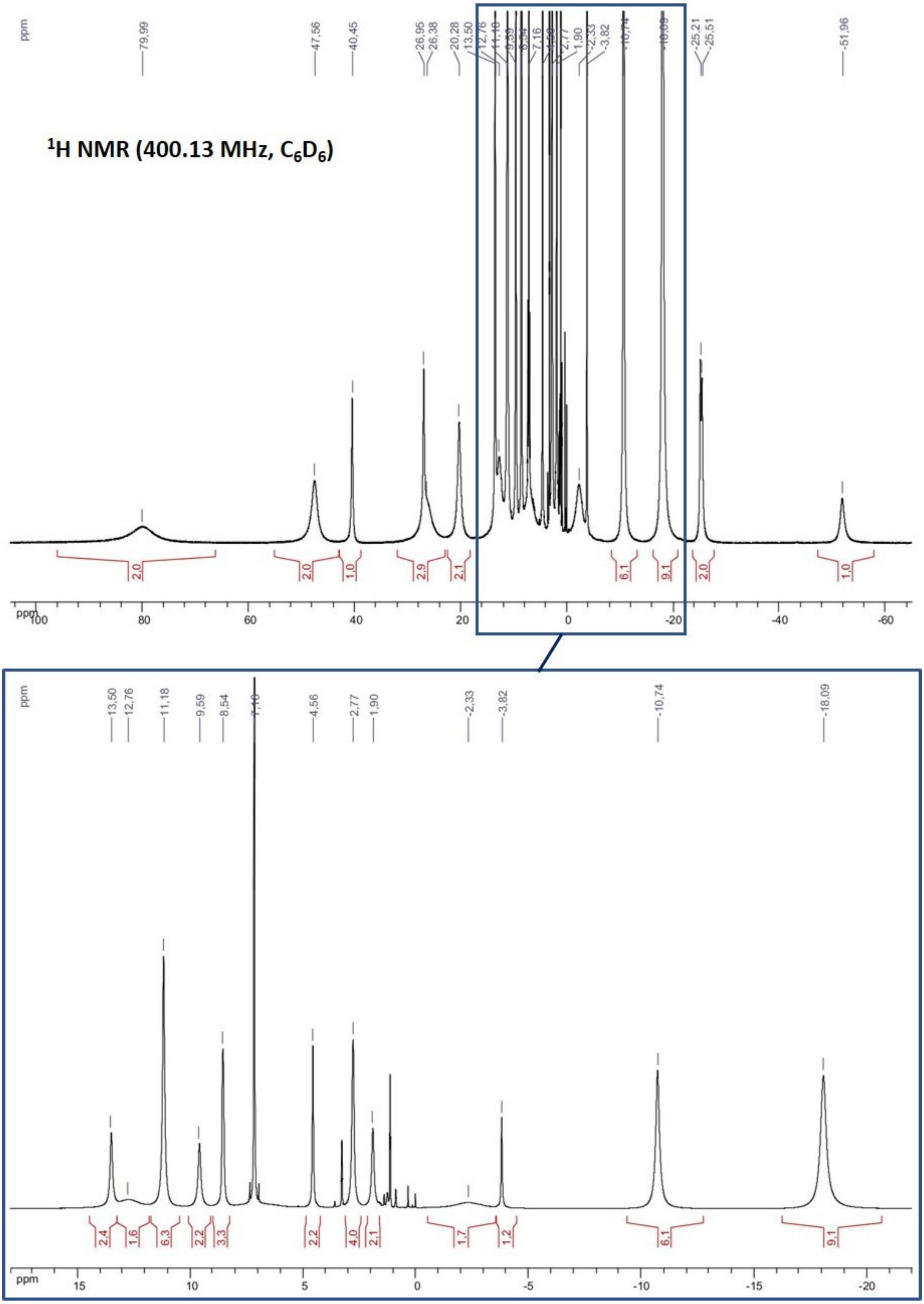

Figure S2. ^1H NMR spectrum of **3** in C_6D_6 (residual protio solvent from C_6D_6 at δ 7.16).

III.3. Complex 4

^{1}H NMR (500.13 MHz, C_6D_6)

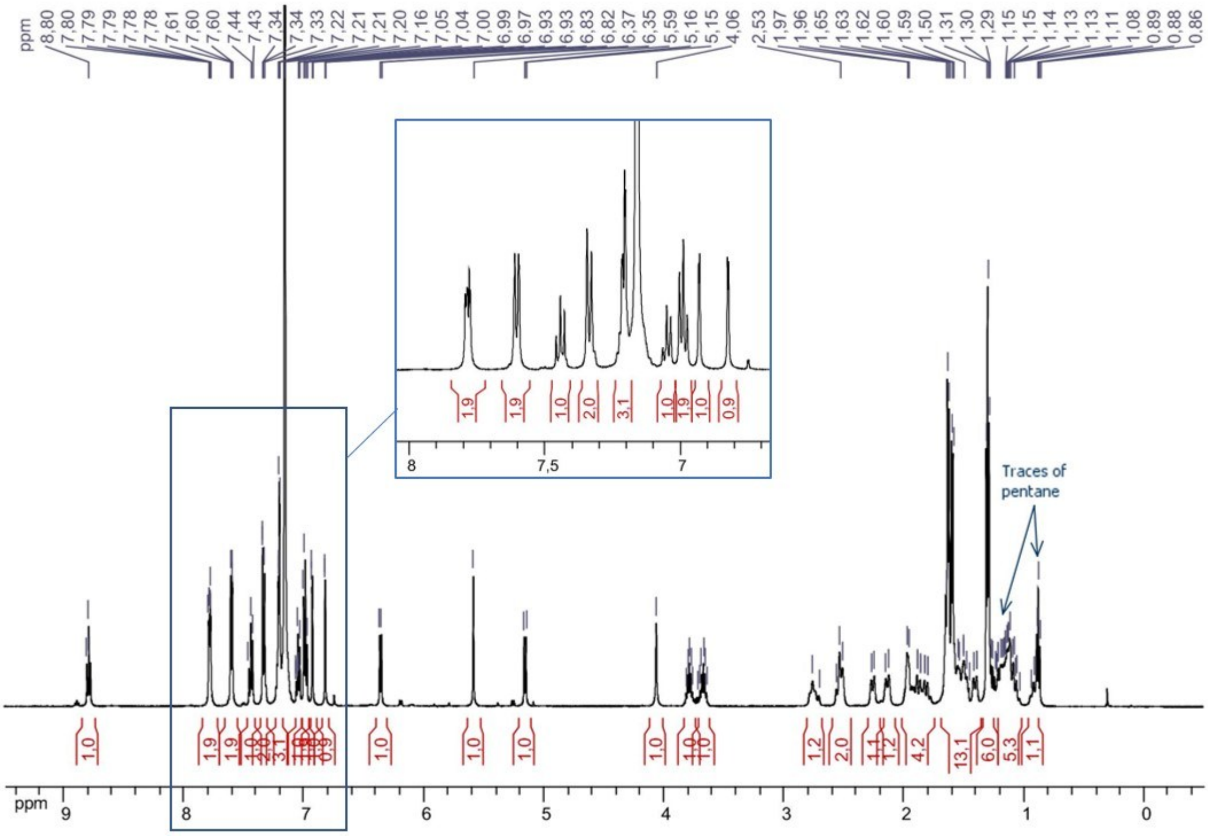

Figure S3. ^{1}H NMR spectrum of **4** in C_6D_6 (residual protio solvent from CD_6 at δ 7.16). Traces of pentane can be seen on the spectrum.

$^{31}P\{^1H\}$ NMR (161.98 MHz, C_6D_6)

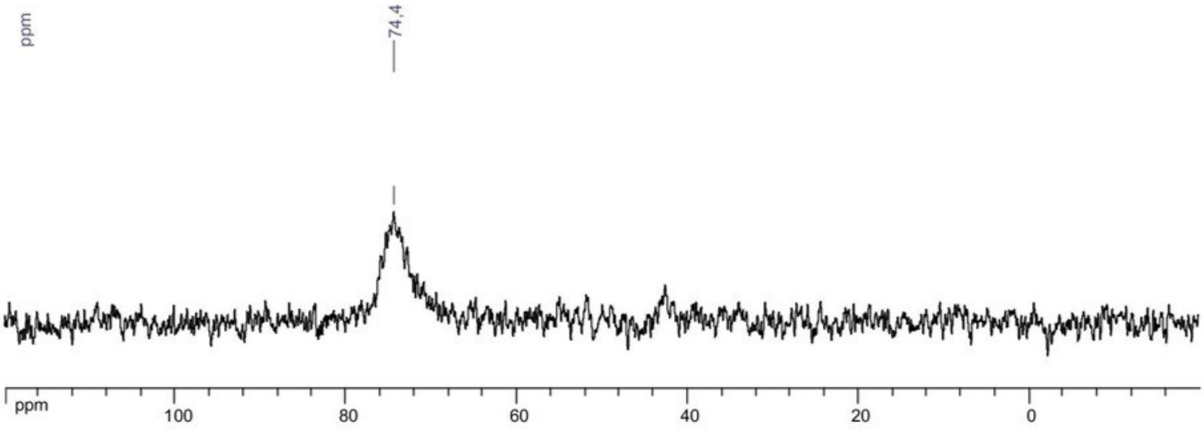

Figure S4. $^{31}P\{^1H\}$ NMR spectra of **4** in C_6D_6.

$^{13}C\{^1H\}$ NMR (125.77 MHz, C_6D_6)

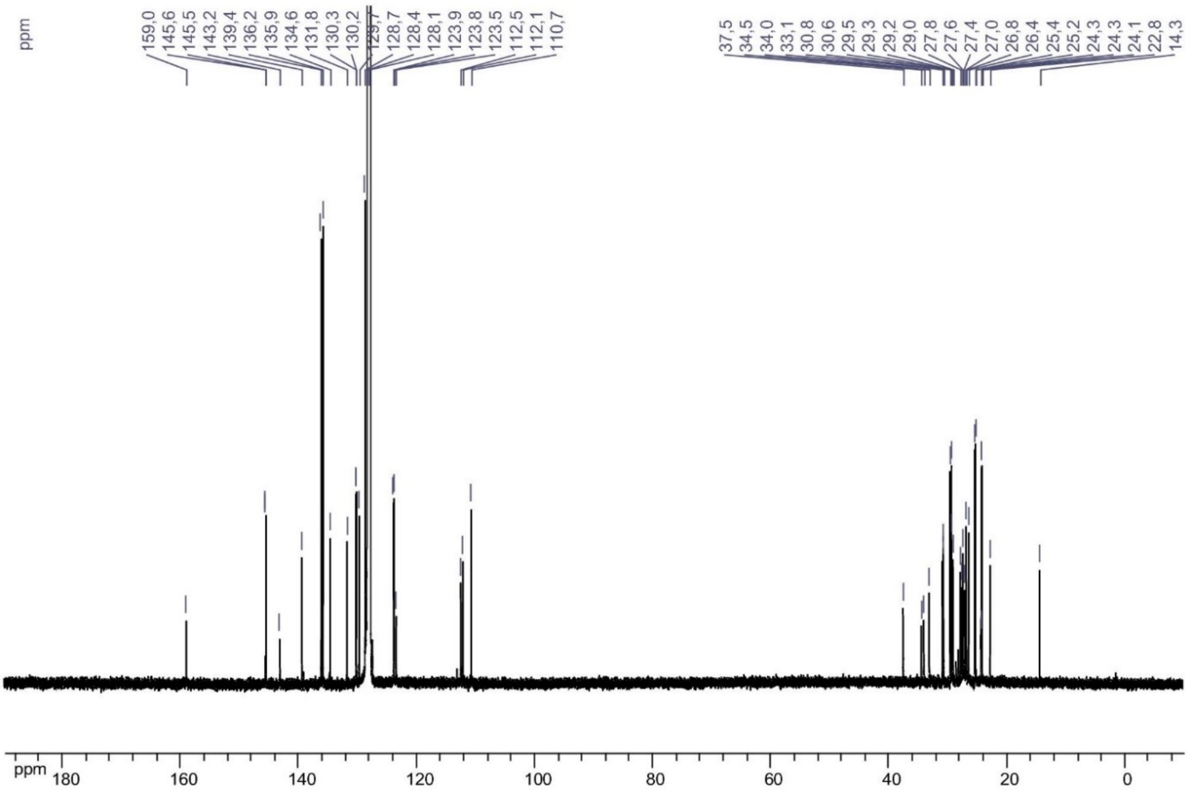

Figure S5. $^{13}C\{^1H\}$ (bottom) and ^{13}C-DEPT (top) NMR spectra of **4** in C_6D_6 (solvent signals at δ 128.06). Traces of pentane can be seen on the spectrum at δ 34.5, 22.8 and 14.3.

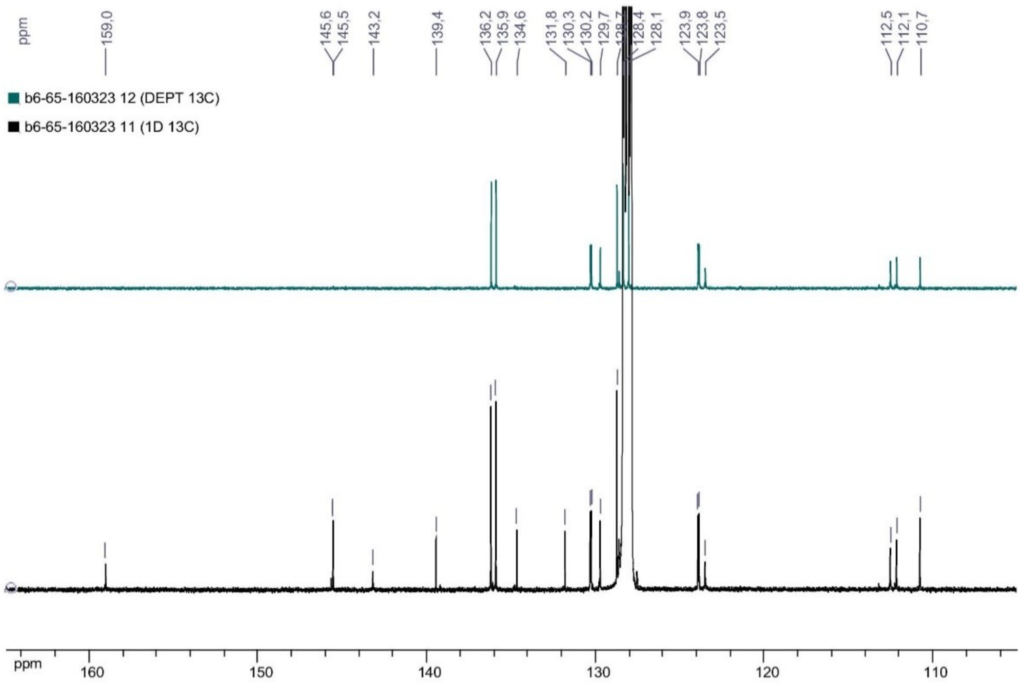

Figure S6. Detail of the region δ 165 – 105 ppm in the $^{13}C\{^1H\}$ (bottom) and ^{13}C-DEPT (top) NMR spectra of **4** in C_6D_6 (solvent signals at δ 128.06).

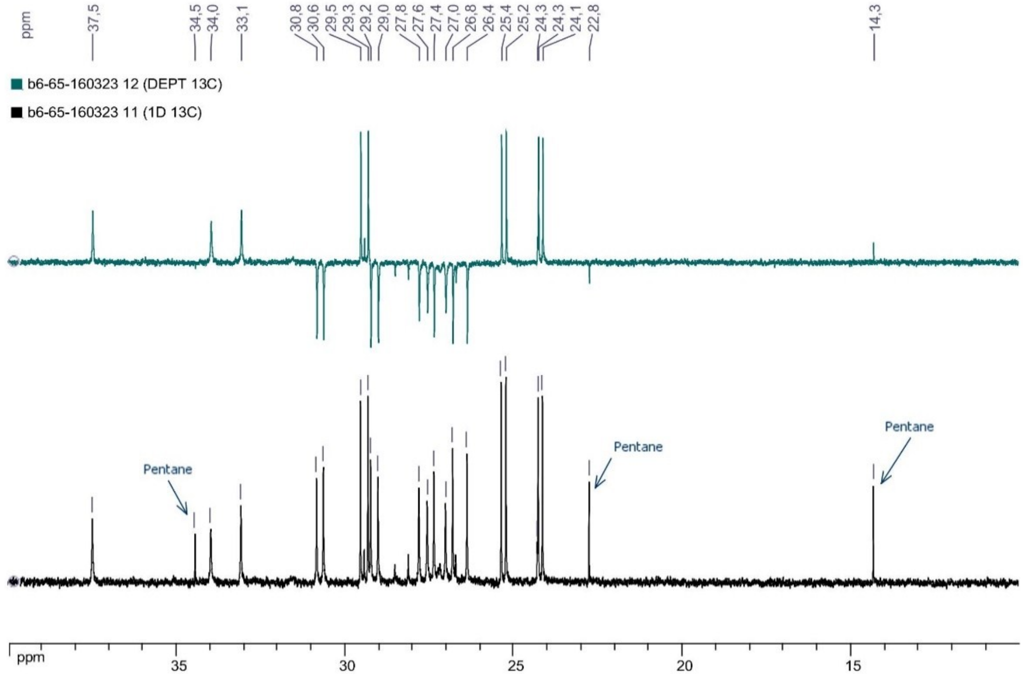

Figure S7. Detail of the region δ 40 – 10 ppm in the $^{13}C\{^1H\}$ (bottom) and ^{13}C-DEPT (top) NMR spectra of **4** in C_6D_6 (solvent signals at δ 128.06). Traces of pentane can be seen on the spectrum.

III.4. ^{1}H NMR spectrum after reaction of 1 with 1 equiv H_2SiPh_2

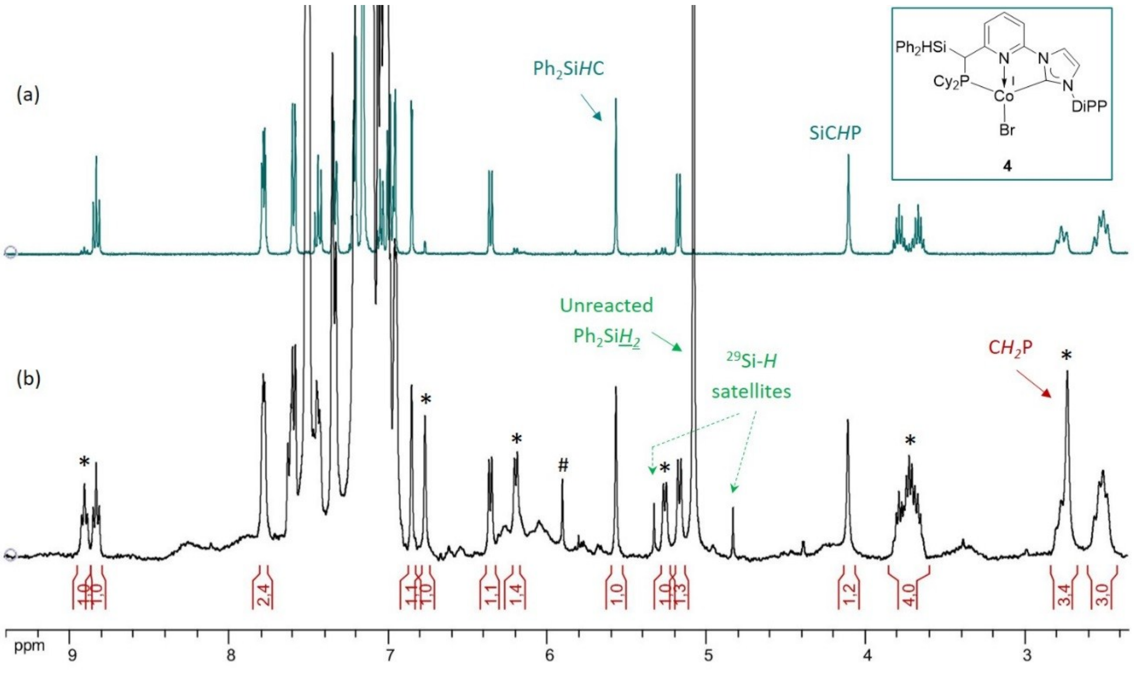

Figure S8. Comparison of the ^1H NMR spectra (range δ 9.4 – 2.3 ppm) of isolated **4** (a) and of the crude product obtained after reaction of **1** with 1 equiv H_2SiPh_2 (b). The * sign corresponds to the second compound formed, assigned to **5** in the main text; # corresponds to an unidentified impurity

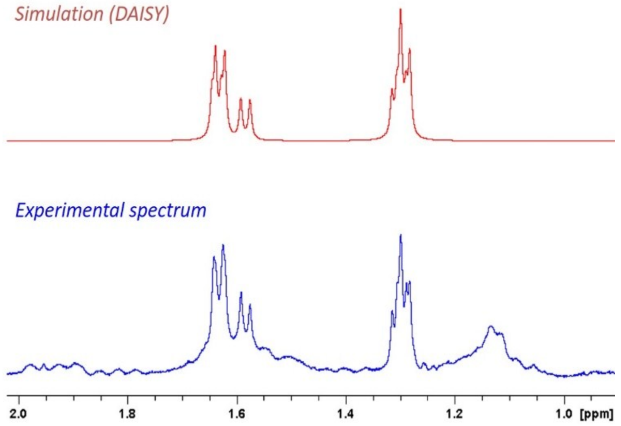

Parameters:

1.635 (d, $^3J_{HH}$ = 6.9 Hz, 6H, CH(CH_3)$_2$ of **5**),
1.629 (d, $^3J_{HH}$ = 6.9 Hz, 3H, CH(CH_3)$_2$ of **4**),
1.583 (d, $^3J_{HH}$ = 6.9 Hz, 3H, CH(CH_3)$_2$ of **4**),
1.306 (d, $^3J_{HH}$ = 6.9 Hz, 6H, CH(CH_3)$_2$ of **4**),
1.297 (d, $^3J_{HH}$ = 6.9 Hz, 6H, CH(CH_3)$_2$ of **4**),
1.290 (d, $^3J_{HH}$ = 6.9 Hz, 6H, CH(CH_3)$_2$ of **5**)

Figure S9. Detail of ^{1}H NMR spectrum in the δ 2.0 – 1.0 ppm region after reaction of **1** with 1 equiv H_2SiPh_2 and simulated spectrum using the DAISY module of the Topspin software (BRUCKER).

III.5. ^{1}H NMR monitoring of the reaction of 1 with excess H_2SiPh_2

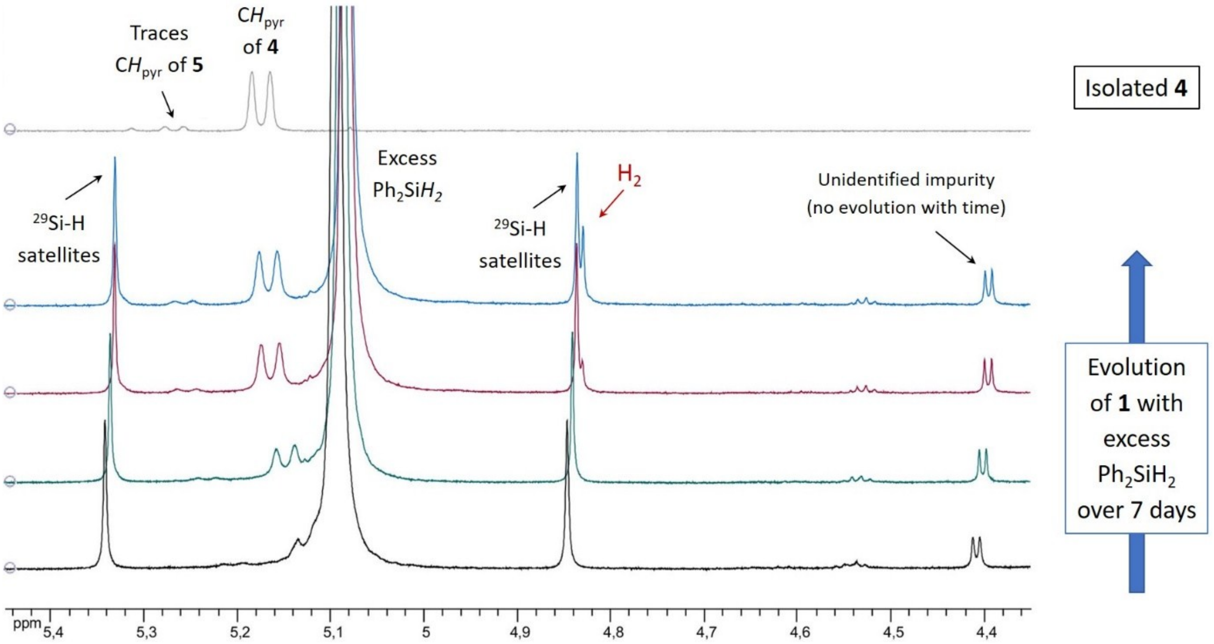

Figure S10. Detail of ^{1}H NMR spectrum in the δ 5.5 – 4.3 ppm region after reaction of **1** with excess H_2SiPh_2. The singlet arising at δ 4.83 ppm can be assigned to H_2 build-up.

IV. EPR SPECTROSCOPY

The EPR spectra of a mixture containing compounds **1** and **2** (non-crystallised batch obtained after reaction between $(^{Cy}PN^{pyr}C^{im})Br$ and $[Co\{N(SiMe_3)_2\}_2]$ in THF at room temperature) in a frozen toluene/ether (1:1) solution ($6x10^{-3}$ M) were first recorded at low temperature. The EPR spectrum at 4 K corresponds to the superimposition of the two species, as shown in Figure S11. The signal for species **2** is centred around 330 mT with seven lines due to the coupling of the unpaired electron with the ^{59}Co nucleus ($I = 7/2$, 100% natural abundance) whereas the signals assigned to species **1** are indicated with arrows. Note that at low field the hyperfine coupling constant of the ^{59}Co nucleus of **1** is less resolved than when the sample has been recrystallized as the concentration is lower (10^{-3}) (Figure 3 in the text). As the temperature increases from 4 K to 70 K, the signal of **1** disappears, which confirmed the presence of two species with different time relaxations.

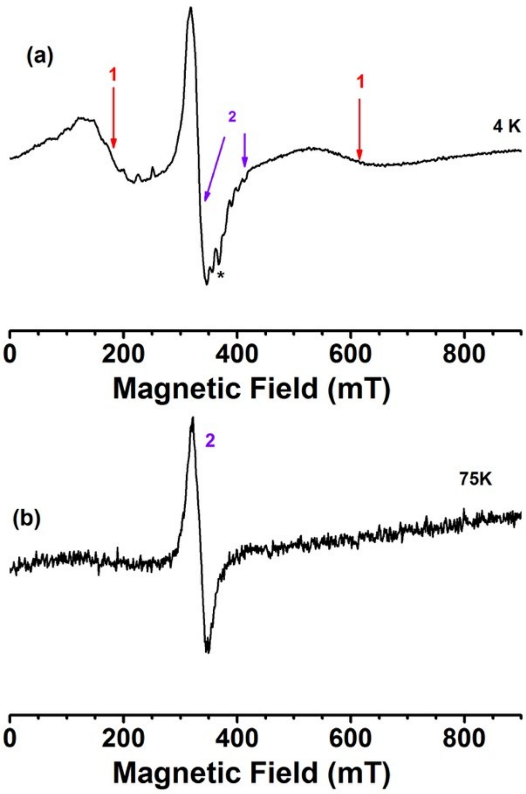

Figure S11. X-band EPR spectra of a mixture of **1** and **2** in toluene/ether (1:1) at low temperature: (a) at 4 K (b) at 70 K. The transition with an asterisk is due to an impurity in the EPR cavity.

V. REFERENCES

1. T. Simler, P. Braunstein and A. A. Danopoulos, *Chem. Commun.*, 2016, **52**, 2717-2720.
2. (a) D. F. Evans, *J. Chem. Soc.*, 1959, 2003-2005; (b) E. M. Schubert, *J. Chem. Educ.*, 1992, **69**, 62.
3. D. H. Grant, *J. Chem. Educ.*, 1995, **72**, 39-40.
4. G. A. Bain and J. F. Berry, *J. Chem. Educ.*, 2008, **85**, 532-536.
5. *APEX2*, *SAINT* and *SADABS*, Bruker AXS Inc., Madison, Wisconsin, USA, 2009.
6. (a) G. M. Sheldrick, *Acta Crystallogr., Sect. A*, 2008, **64**, 112-122; (b) G. M. Sheldrick, *SHELX2013*, University of Göttingen, Germany, 2013.